Adsorption (2009) 15: 507–519
DOI 10.1007/s10450-009-9201-x

Porosity characteristics and pore developments of various particle sizes palm kernel shells activated carbon (PKSAC) and its potential applications

S.M. Mak · B.T. Tey · K.Y. Cheah · W.L. Siew · K.K. Tan

Received: 26 June 2008 / Accepted: 12 November 2009 / Published online: 25 November 2009

Abstract The adsorption behaviour and the micro- and mesopore size distributions of commercial palm kernel shell activated carbons (PKSAC) and other commercial activated carbon are characterized. The results showed that PKSAC are predominantly microporous materials, where micropores account 68–79% of total porosity. On the other hand, commercial activated carbons: Norit SX Plus, Calgon 12 × 40, and Shirasagi "A" activated carbons contained high mesopore fraction ranging from 33 to 52%. The analysis showed that the degree of mesoporosity of PKSAC is increased steadily with the decrease of particle size. This is due to the presence of channels interconnect the smaller pores in the interior of smaller particle size PKSAC. The smaller size PKSAC particle that is highly mesoporous has preformed better on the adsorption of larger molecules such as methylene blue. On the other hand, bigger size PKSAC particle has better performance on the adsorption of smaller adsorbates such as iodine.

Keywords Palm kernel shell activated carbons · Nanoporous · Mesoporosity · Particle size · Adsorption · Diffusion

S.M. Mak · B.T. Tey
Department of Chemical and Environmental Engineering, Faculty of Engineering, Universiti Putra Malaysia, 43400 Serdang, Malaysia

K.Y. Cheah · W.L. Siew
Malaysian Palm Oil Board, Persiaran Institusi Bandar Baru Bangi, 43000 Kajang, Malaysia

K.K. Tan (✉)
HELP University College, BZ-2 Pusat Bandar Damansara, 50490 Kuala Lumpur, Malaysia
e-mail: tankk@help.edu.my

Nomenclature

q_t	Amount of methylene blue ions adsorbed at time t (mg/g)
Q^0	Number of moles of solute adsorbed per unit weight of activated carbon (mol/g)
A_M	Cross sectional area of one MB ion (m^2)
b	Energy of adsorption constant of Langmuir model
C_e	Solute concentration in the aqueous phase at time t (mg/L)
C_0	Initial solute concentration in the aqueous phase (mg/L)
D_{meso}	Average mesopore diameter determined by BJH model (Å)
D_{micro}	Mean micropore diameter determined by HK model (Å)
K_F	Freundlich isotherm equation constant $[mg/g(1/mg)^{1/n}]$
k_f	Rate constant of pseudo-first-order equation defined in (4) (min^{-1})
k_i	Rate parameter of intraparticle diffusion defined in (6) ($mg\,L^{-1}\,min^{-1}$)
k_s	Rate constant of pseudo-second order equation defined in (5) ($L\,mg^{-1}.min^{-1}$)
N_a	Avogrado's number (6.023×10^{23})
$1/n$	Freundlich isotherm equation constant (dimensionless)
q_e	Amount of methylene blue ions adsorbed at equilibrium (mg/g)
R^2	Regression factor of sorption kinetic plots
S_{BET}	BET specific surface of activated carbon (m^2/g)
S_{MB}	Surface coverage of methylene blue ions within activated carbon (m^2/g)
S_{micro}	Surface area of activated carbon due to micropores (m^2/g)
t	Time (min)

V_{meso} Mesopore volume obtained by BJH model (cm^3/g)
V_{micro} Micropore volume obtained by DR model (cm^3/g)
V_t Total pore volume of activated carbon (cm^3/g)
X_{MB} Fraction of surface coverage of methylene blue ions over BET surface area (S_{MB}/S_{BET})

1 Introduction

Activated carbons are widely used in many industrial processes such as separation and purification of gas mixtures, selective adsorption, storage of compressed natural gas, and other novel applications such as catalyst supports. High internal surface area and well-developed porosity are the key properties to provide feasible utilization of these materials in specific commercial applications. The understanding on the impact of micro- and mesopore size distribution on the adsorption capacity of the activated carbons is important prior to its commercial applications. For instances, the extent of mesoporosity is an important criterion used to select the activated carbon for the adsorption treatments to removal the liquid phase contaminants (Pelekani and Snoeyink 1999; Hsieh and Teng 2000). However, in the applications of gas separations and storage, highly microporous activated carbon is preferred. It has been reported that highly nanoporous activated carbons with pore size range of 5 to 7 Å (Sircar et al. 1996) and 11 to 12 Å (Safanova et al. 2000) have shown remarkable performances in separation and purification of gas mixtures and storage of natural gas.

The productions of activated carbons with good adsorption properties from various waste products other than bituminous and coal are of interest in the present day. In Malaysia, abundantly available of palm kernel shells have promote its use as precursor for the production of activated carbons. Commercial steam-activation of carbonized palm kernel shell has yielded highly nanoporous activated carbons comprising both micro- and mesopores. Textural properties such as micropore volume (V_{micro}), and mesopore volume (V_{meso}), micro- and mesopore size distribution were found to differ according to particle sizes as determined by nitrogen physisorption.

In many commercial adsorption processes, the transport of adsorbates molecules into the porous interior of activated carbons implies limitations in the overall rate of adsorption especially in fixed bed applications. This is mainly due to the polydispersed and randomly arranged of pores in a carbon particle. Consequently, adsorption of adsorbates molecules into the interior void surfaces is a diffusion controlled mechanism. The pore and surface diffusion mechanisms have been associated to the adsorption phenomena either individually or simultaneously. Both mass transfer mechanisms assume the conservation of Ficks's law. The pore diffusion mechanism involves the diffusion of adsorbates through the pore fluid due to the presence of radial concentration gradient. The magnitude of surface diffusion flux is characterized by surface diffusivity, which is known to vary with both temperature and the extent of coverage (Tien 1994). However, it is difficult to determine the transport coefficient in activated carbons due to the irregularity of the pore structure. The irregularity of the pore structure has enhanced the energetic heterogeneity of the surface and thus making the nature of surface diffusion complicated (Prasetyo et al. 2002). On the other hand, if the pore radius is less than the mean free path of the fluid molecules, collision of fluid molecules with the pore surface may dominate, hence, resulting in Knudsen diffusion. Nevertheless, in reality, diffusion occurs in pore space where the actual path is zigzag and randomly arranged, hence incorporating the tortuousity factor of higher values as compared to other adsorbents such as silica and alumina (Prasetyo et al. 2002; Tien 1994).

Therefore, many complex mathematical models have been developed to address the transport of molecules in highly porous adsorbents such as the heterogeneous diffusion model (Hu and Do 1994; Do and Wang 1998) and pore diffusion model (Chen et al. 2001; Pritzker 2003). However, the mathematical complexity of the rigid models incurred inconvenience for practical applications (Guibal et al. 1998; Wu et al. 2001). Nevertheless, in this present study, three simplified sorption kinetics models of pseudo-first, pseudo-second and intraparticle diffusion are employed to determine the rate-controlling step in the adsorption phenomena.

Successful conversion of activated carbons from palm kernel shells and its application in gas and liquid adsorption have been achieved and reported by several researchers (Luo and Guo 2001, 2003; Luo and Jia 2007; Tan et al. 2008). However, the porosity characteristics and pore developments of palm kernel shells activated carbon (PKSAC) are not well understood. Luo and Guo (2001) reported that the BET surface area and microporosity of OPSA are strongly affected by the activation temperature and activation time. The performance of an activated carbon in various applications generally depends on the porosity within the particle. Information on the volume and pore size distribution would allow rationalization of the practicality of the activated carbon in a particular application. The objective of this study is to investigate the porosity characteristics and pore developments of various particle sizes of palm kernel shells activated carbon (PKSAC) and its potential applications. The analysis shows that the degree of mesoporosity of PKSAC increases steadily with the decrease of particle size. Scanning electron microscopy is used to illustrate the differences of structural and surface morphology of the PKSACs and other commercial activated carbons. The influence of irregular pore structures on the adsorption capacities and sorption kinetics of PKSACs are included in this study in order to

provide information for its future commercial utilization. Finally, the performance of PKSACs in the bleaching of glycerine is determined. Other commonly applied commercial activated carbons are selectively included for comparison.

2 Experimental

2.1 Physisorption analysis of activated carbons

The commercial steam-activated PKSACs are provided by KDTech. Sdn Bhd (Klang, Malaysia). These PKSACs are produced by steam-activation at temperature of approximately 1000 °C in a horizontal rotary kiln with heat-recovery system. These activated carbons are classified accordingly to the particle size, 1.7–2.38 mm (PKSAC1), 0.6–1.7 mm (PKSAC2), 0.25–0.6 mm (PKSAC3), 0.15–0.3 mm (PKSAC4) and less than 0.15 mm (PKSAC5). All PKSACs possessed iodine numbers in the range of 1000–1100 mg/g. Physical characterization of other commercial activated carbons such as powder-based Norit SX Plus (NP) (Norit, The Netherlands), Shirasagi "A" (SA) (Shirasagi, Japan) and granular Calgon 12 × 40 (CA) (Calgon, USA) are included to compare the difference in porosity and resulting sorption behaviour.

All samples were heated in the furnace at 200 °C overnight to eliminate the moisture content in samples. Representative samples typically of 0.1–0.2 g were degassed to a residual pressure of 1–2 μm Hg by heating at 200 °C for at least 24 hr (Micromeritics, Model ASAP 2010) prior to nitrogen adsorption measurements. The adsorption isotherms were measured under the relative pressure range of 10^{-6} to 1. The adsorption-desorption isotherms were interpreted by the application of modified Brunnauer-Emmet-Teller (BET) method (Brunauer et al. 1938) for surface area (S_{BET}) calculation by using nitrogen molecule surface area of 0.162 nm^2. The total pore volume (V_t) was estimated at relative pressure of 0.99. The V_{micro} was calculated using the Dubinin-Raduschkevich (DR) equation (Dubinin 1989). V_{meso} and mesopore average diameter (D_{meso}) were obtained using the Barret-Joyner-Halenda (BJH) method (Barret et al. 1951). The median pore diameter of micropores (D_{micro}) was calculated using Horvath-Kawazoe (HK) equation (Harkins and Jura 1944).

2.2 Surface topography of PKSACs

The microstructure of the PKSACs (PKSAC1, 2 and 3) and NP were examined using a scanning electron microscope (SEM) (Hitachi-S2700). Samples for optical microscopy were gold sputter coated prior to analyses. High-resolution magnification within the range of 60 to 20 K times under controlled vacuum condition. SEM analyses enable direct observation of the surface characteristics of the carbons as well as the homogeneity or heterogeneity of the carbons structures.

2.3 Experimental procedures for the adsorption of MB and iodine

Reagent grade iodine and MB supplied by Fischer Chemicals (UK) were employed as adsorbates in the liquid phase adsorption experiments at ambient temperature. Each of the adsorption experiments described employs a synthetic aqueous solution of MB (3,7 bis (dimethylamino) phenothiazin-5-ium ion) with molecular weight of 373.9 g/mol as test solution (D'Silva 1998; Gergova et al. 1993; Kaewprasit et al. 1998; McKay et al. 1999). The concentrations of MB solutions were analyzed by using Cintra 5 ultra-violet/visible double beam spectrophotometer. A calibration curve of optical densities against MB concentrations ($R^2 = 0.9994$) was obtained by using standard MB solutions of known concentrations. Batch adsorption tests were carried out by placing certain amount of PKSAC2, PKSAC5 and NP in 20 mL of MB solution and agitated at 150 rpm. Adsorption kinetics are evaluated by contacting 0.01 g of activated carbon sample in varied initial concentrations of 100, 250 and 500 mg/L. Samples are collected at intervals of 2 to 240 minutes. To determine the maximum sorption capacities of MB, 0.1 g of activated carbon samples were equilibrated for 4 hours in 20 mL of different concentrations of MB solutions, 250, 500, 1000, 2500 and 5000 mg/L. Effect of adsorbent dosage is determined by placing different mass of activated carbons, of 0.2, 0.5 and 1.0 g in 20 mL of 5000 mg/L MB solution and agitated at 150 rpm for 4 hours. The extent of iodine adsorption for activated carbon samples of PKSAC1, PKSAC2, PKSAC5 and NP are carried out to elucidate the influence of microporosity on the adsorption behaviour of these structures. Batch adsorption of iodine is conducted by using solution of iodine prepared by dissolving iodine in potassium iodide (I_2/KI). Different weights of activated carbon samples from 0.05 to 0.5 g were added to 25 mL of 0.05 $mol.dm^{-3}$ solution of I_2/KI and agitated at 150 rpm for 4 hours.

2.4 Experimental procedures for the bleaching of glycerine

Activated carbons of 0.1, 0.5, 1 and 5 weight % are employed in batch bleaching of glycerine. Samples of activated carbons evaluated are PKSAC2, PKSAC4, PKSAC5, SA and CA. Appropriate amount of activated carbon samples are added to 50 mL of glycerine with APHA (American Public Health Association) colour of more than 30. Temperature of slurry is maintained in the range of 65 to 75 °C in a water bath and agitated for 1 hour. Activated carbons are then removed by filtration. The colour of bleached glycerine is determined by using LICO 300 by employing the Hazen-colour value or APHA-method (DIN-ISO 6271).

3 Results and discussion

3.1 Physical properties of activated carbons

Nitrogen adsorption isotherms of all activated carbons are shown in Fig. 1. PKSAC1-5 and CA exhibited type-I adsorption isotherms, which indicate the microporous nature of these carbons. This is characterized by the sharp curve at very low relative pressure, which subsequently levels off to a long nearly horizontal section. The occurrence of slight hysteresis simultaneously indicates the presence of mesopores. Isotherms of NP and SA resemble a combination of types II and I with prominent hysteresis loops of type H4 (according to IUPAC classification of hysteresis loops), which occur in the region of 0.3 to 1 P/P_0. This shows the higher degree of mesoporosity contained in both structures as compared to PKSAC and CA.

The micro- and mesopore size distributions of all activated carbons are shown in Figs. 2 and 3, respectively. The physical properties of the activated carbons, S_{BET}, V_{micro}, V_{meso}, D_{micro}, D_{meso} and V_t are listed in Table 1. All activated carbons consist of micropores with almost similar pore diameter, which falls within the narrow range of 5.5 to 6.4 Å. PKSAC are predominantly microporous materials, where micropores account 68–72% of total porosity. On the other hand, NP and CA contained higher mesopore fraction of 52 and 36%, respectively. An interesting porosity trend is observed in PKSAC of decreasing particle size. The degree of mesoporosity is found to increase steadily with the decrease in particle size. Hence, PKSAC5 possessed higher mesopore fraction of 33% than PKSAC1-4. The median pore diameter of mesopores of PKSAC5 is higher than other PKSACs.

Electron micrographs of granular PKSAC depict the phenomena of pore channelling as shown in Fig. 4. Large crevices or slits were observed on the surface of a single particle (Fig. 4a). Figure 4b shows that these large openings serve as a passageway to the abundant micro- and mesopores located in the internal structure of the PKSAC. This resulted in a polydispersed capillary structure as shown in Fig. 4c, where random displacements of these channels occurred within the particle resulted the pore channelling effect in PKSAC (Fig. 4d). Figure 5 shows that the surface characteristics of NP appear to be homogeneous with fracture-like structures as similarly observed by Kluson and Scaife (2001). Figure 6 exhibits the surface morphology of CA, consisting of large pores at the surface. The apparent difference between the microstructures is related to the characteristics of the precursor as well as the selective removal of the graphitic plates towards the mechanism of steam diffusion. This is due to the heterogeneous reaction of water vapour with carbon particles, which is coherently governed, by the chemical reaction of gases with the solid surface inside the particles and diffusion mass transfer through the porous structure of the particle (Laurendeau 1978). The PKSAC are produced by steam-activation at temperature of approximately 1000 °C from palm kernel shell, while NP is prepared via acid washed and steam activation from coal and CA is prepared by heating the coal in an oxygen free environment and subsequently activated by additional heating in the presence of oxygen and steam.

Thorough characterization of the PKSACs illuminated the distinguished difference in porosity of PKSACs with

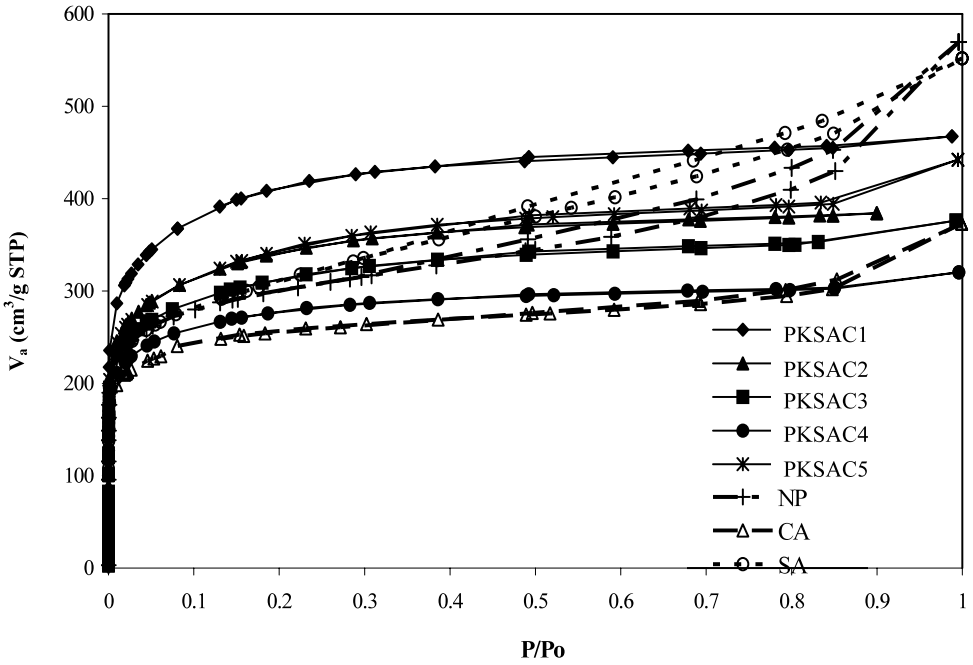

Fig. 1 Adsorption isotherm of nitrogen at 77K of PKSAC1-5, NP, CA and SA

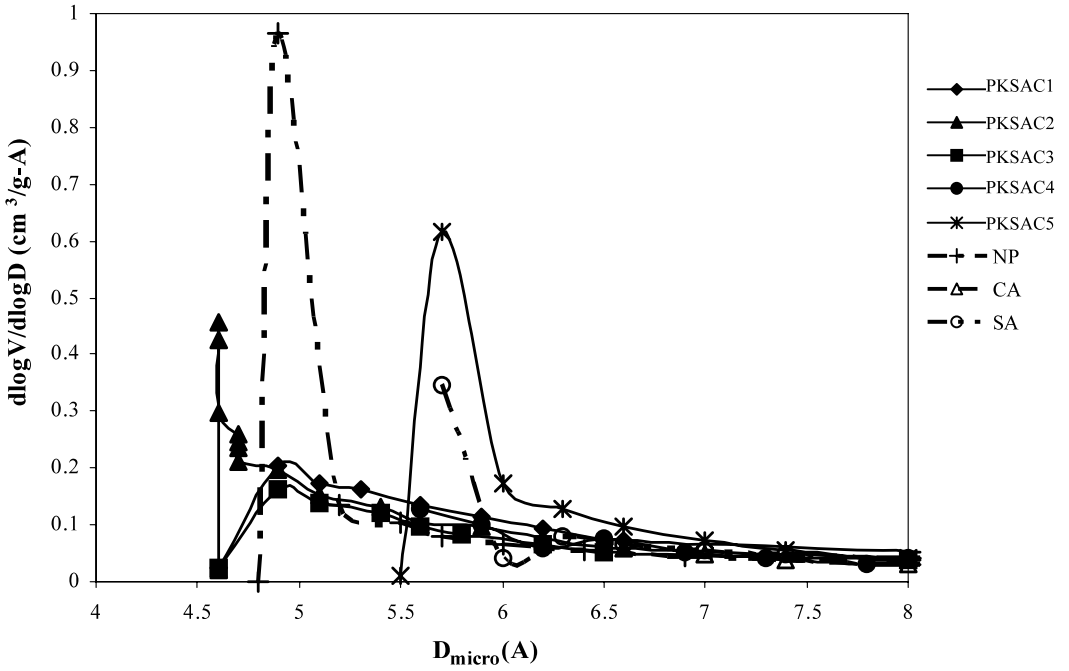

Fig. 2 Micropore size distributions of all activated carbons with mean pore diameter in the range of 5.3 to 6.4 A

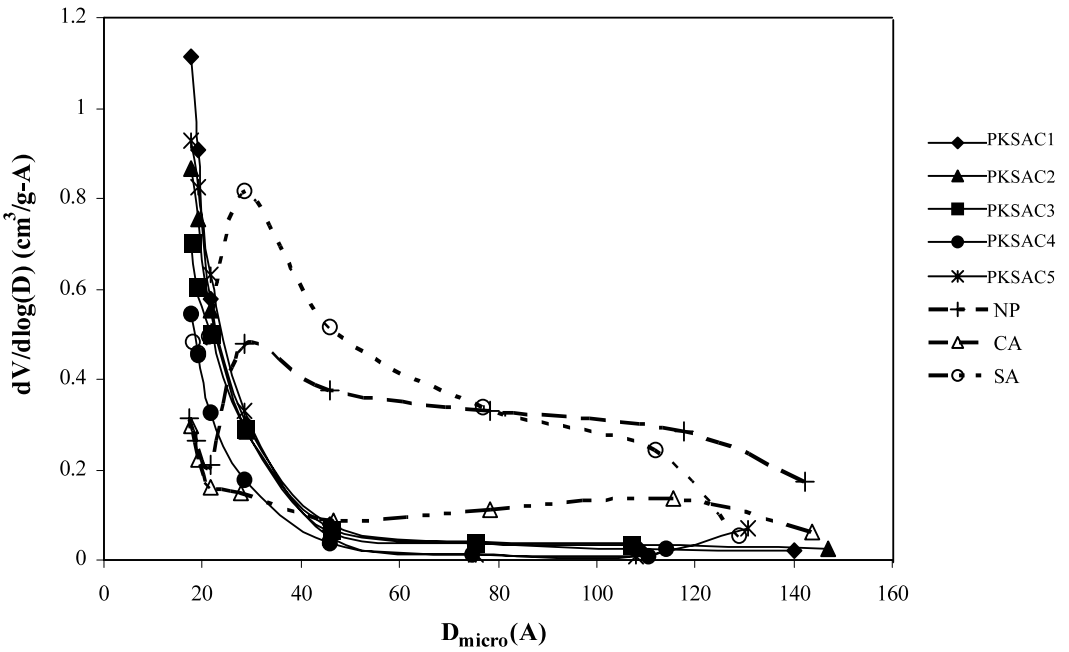

Fig. 3 Mesopore size distribution of all activated carbons

other activated carbons. The influence of the physical parameters attributed by both micro- and mesoporosity would be addressed in the performances of these carbons in liquid phase adsorption tests. This coherently includes the impact of the polydispersed capillary found in PKSACs on the adsorption behaviour.

3.2 Liquid phase adsorption of MB

Adsorption of adsorbates into the porous structures of PKSAC proceeds through sequence of diffusion steps, beginning from the bulk phase and subsequently into the nanopores comprising both micro- and mesopores. The

Table 1 The physical properties of commercial activated carbons

	S_{BET} m^2/g	S_{micro} m^2/g	V_{micro} cm^3/g	V_{meso} cm^3/g	V_t cm^3/g	$\%V_{micro}/V_t$	D_{micro} Å	D_{meso} Å
PKSAC1	1599	879.8	0.56	0.11	0.722	77.6	5.5	26.0
PKSAC2	1237	834.7	0.47	0.09	0.595	79.0	5.3	24.8
PKSAC3	1146	828.4	0.43	0.12	0.582	73.9	5.3	26.1
PKSAC4	1190	825.7	0.45	0.21	0.590	76.3	6.0	29.0
PKSAC5	1234	800.7	0.46	0.30	0.680	67.7	6.4	32.6
NP	1115	798.1	0.42	0.48	0.881	47.7	6.3	57.1
CA	959	737.8	0.37	0.25	0.58	64.0	5.8	57
SA	1120	674.8	0.43	0.60	0.64	67.2	6.4	42

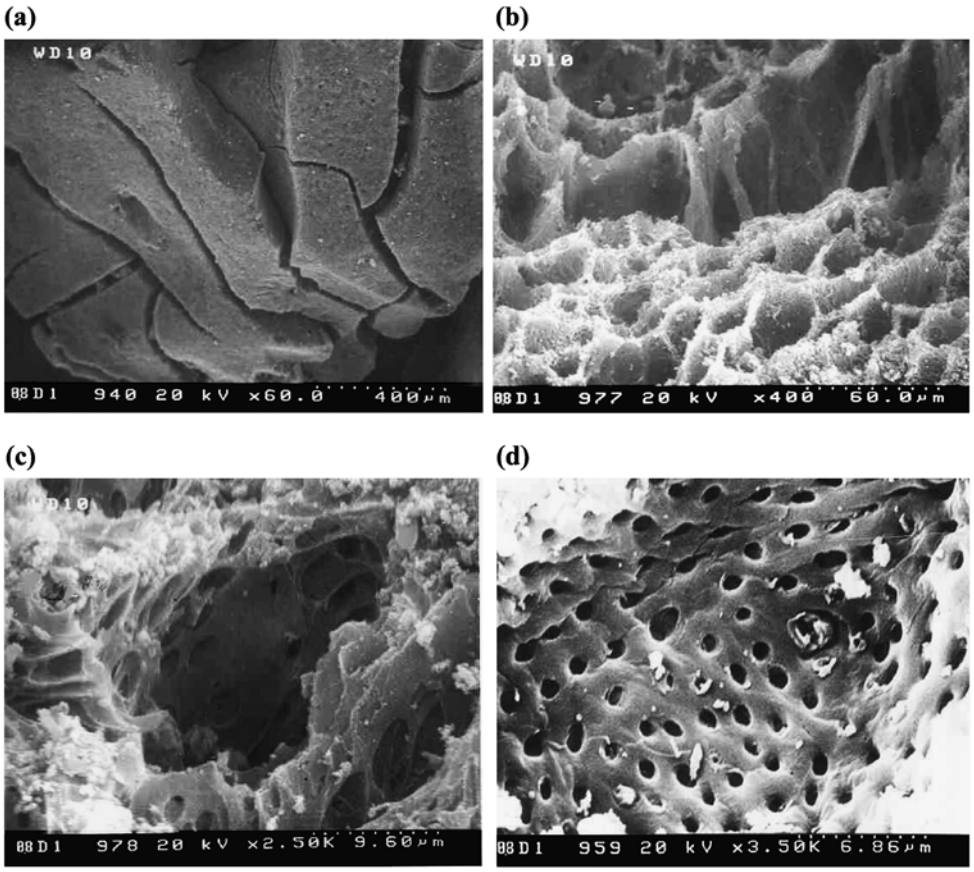

Fig. 4 Micrograph of granular PKSAC of (**a**) 60x magnification. (**b**) 400x magnification. (**c**) 2.5 Kx magnification. And (**d**) 3.5 Kx magnification

length of diffusion would predominantly determine the extent of fractional coverage in the micropore region (Teng and Hsieh 1998). These micropores provide the major adsorptive sites in aqueous solutions while weaker adsorption occurs in the mesopores (Yang et al. 1993). Nevertheless, aggregation of these adsorbates in the smaller cross-sectional capillaries will cause detrimental effect of pore blockage, thus, resulting in incomplete utilization of the internal surface area of the micropores (Hsieh and Teng 2000; Teng and Hsieh 1998; Pelekani and Snoeyink 1999). Longer diffusion path may incur in higher probability of pore blockage and hence, smaller coverage of micropore fraction.

Two PKSACs with different mesoporosity, PKSAC2 (15% mesoporosity) and PKSAC5 (44% mesoporosity) were used to elucidate the role of mesopores in the adsorption of MB ions. The typical fraction of dye adsorbed-time profile is shown in Fig. 7. The result showed that PKSAC5 of higher mesoporosity required only one hour's contact time to achieve equilibrium. On the other hand, a relatively longer diffusion time was taken by PKSAC2 system at low concentration of MB (100 mg/L). This might be due to the lower

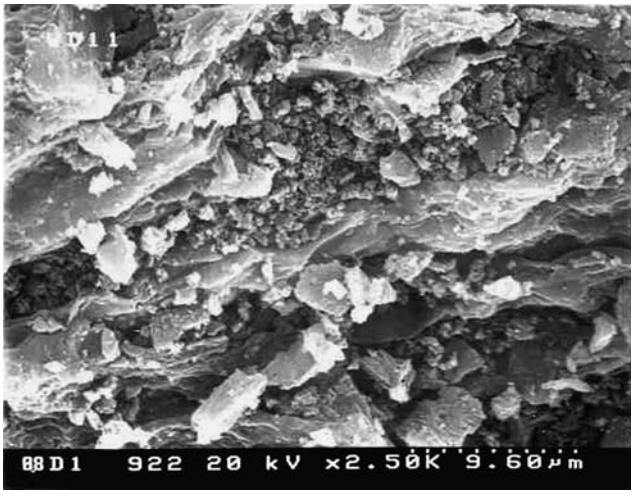

Fig. 5 Micrograph of NP of 2.5 Kx magnification

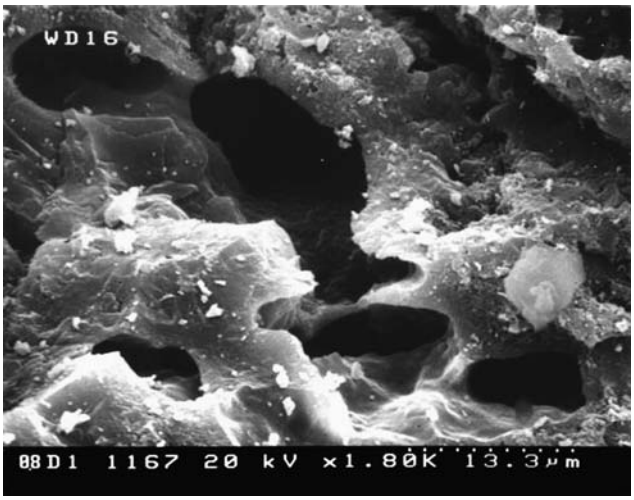

Fig. 6 Micrograph of CA of 1.8 Kx magnification

fraction of mesopores contained in PKSAC2 of 0.09 cm^3/g as compared to PKSAC5 of 0.30 cm^3/g. This implies that the diffusion and adsorption of the large MB ions occur rapidly in the capillaries with average diameter of 32.6 Å in PKSAC5, assuming that larger pores serve as a passageway to the internal smaller pores of approximately 6 Å. Different adsorbent dosages of 0.2, 0.5 and 1 g were employed to determine the economical factor of utilizing these materials. OPSA5 and NP exhibited superior dye removal for all initial concentrations of 1000, 2500 and 5000 mg/L MB solution at low carbon dosage (Fig. 8). However, higher dosage of PKSAC2 of 0.5 g is required to achieve similar performances of PKSAC5 and NP.

3.3 Adsorption isotherm of MB

The well-known Langmuir (1) and Freundlich (2) models are used to determine the maximum adsorption capacity of MB. MB adsorption isotherm data at different initial dye concentrations have been fitted to the linearised form of (1) and (2) expressed as (3) and (4) respectively.

$$q_e = Q^0 b C_e/(1 + bC_e) \tag{1}$$

$$q_e = K_F C_e^{1/n} \tag{2}$$

$$C_e/q_e = 1/Q^0 b + C_e/Q^0 \tag{3}$$

$$\log q_e = \log K_F + (1/n) \log C_e \tag{4}$$

where q_e (mg/g) represents the amount of adsorbed MB per g adsorbent at equilibrium, C_e (mg/L) is the concentration of solute remaining in solution at equilibrium, Q^0 is the number of moles of solute adsorbed per unit weight of adsorbent in forming complete monolayer on the surface and b is the constant related to the energy of the adsorption, K_F

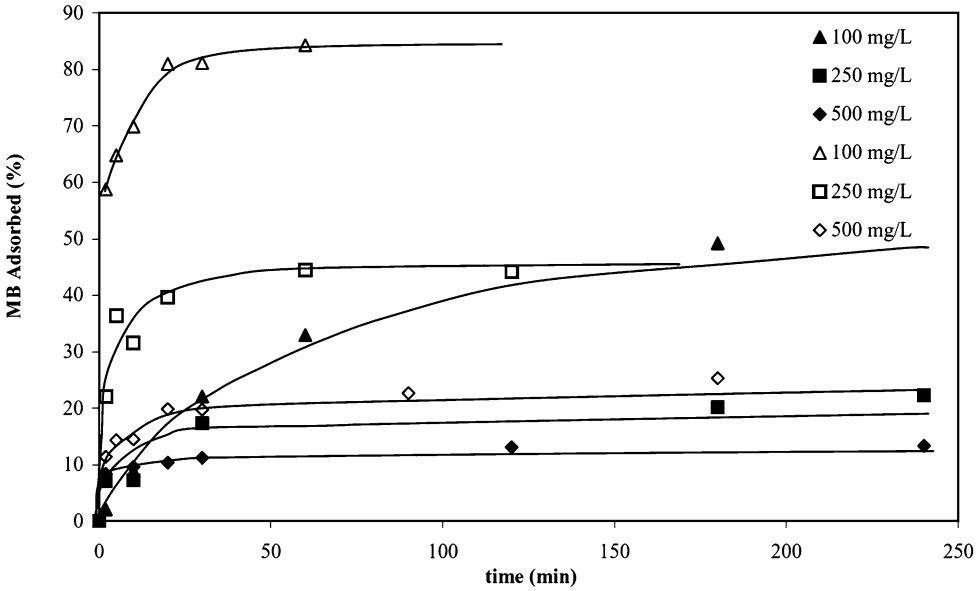

Fig. 7 The adsorbed-time profile for PKSAC2 (*filled series*) and PKSAC5 (*non-filled series*) at different initial concentration of MB solutions

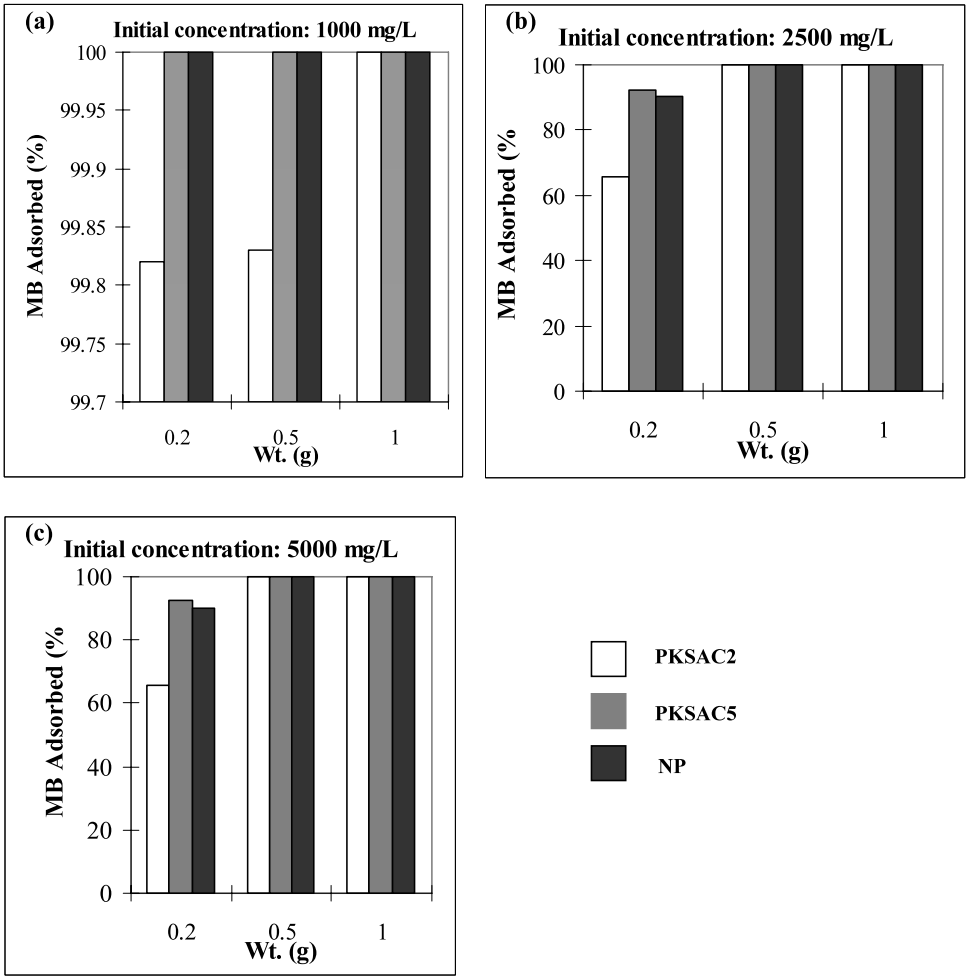

Fig. 8 Effect of activated carbon dosage on the adsorption of MB at higher concentrations of (**a**) 1000, (**b**) 2500 and (**c**) 5000 mg/L

$[\text{mg/g}(1/\text{mg})^{1/n}]$ is the Freundlich isotherm equation constant, and $1/n$ is a measure of the adsorption intensity or surface heterogeneity.

The data of the adsorption of MB for PKSAC2, PKSAC5 and NP are well fixed with Langmuir adsorption equation ($R^2 > 0.994$), but not well fixed with Freundlich equation (R^2 ranging from 0.0616 to 0.9736). The linearised plot of Langmuir adsorption isotherm of MB for PKSAC2, PKSAC5 and NP are depicted in Fig. 9. The comparative adsorption parameters of MB, maximum sorption capacity (Q^0), constant b, Freundlich isotherm equation constants (K_F and $1/n$), specific surface area of MB ions (S_{MB}) and fraction of surface coverage of MB ions over BET surface area (X_{MB}) are listed in Table 2. S_{MB} (D'Silva 1998) is given by the following expression:

$$S_{MB} = Q^0 \cdot N_a \cdot A_M \tag{5}$$

where N_a is the Avogadro number (6.023×10^{23}) and A_M is the cross-sectional area of one adsorbed molecule (m^2) which is taken as 120 $Å^2$ for MB (D'Silva 1998). The value of A_M is calculated based on the assumption that the actual area covered by each molecule is approximately that of the smallest enclosing rectangle or circle where molecules are adsorbed (Gregg and Sing 1967). The increasing order of Q^0 given as PKSAC2 < PKSAC5 < NP, where S_{MB} and X_{MB} were found to increase coherently accordingly to the degree of mesoporosity. This concludes the role of mesoporosity and pore capillaries in facilitating the adsorption of large adsorbates in the highly microporous PKSAC structures. The value of constant b estimated is in the range of 0.13–0.18 l/mg, a value comparable to that estimated in Tan et al. (2008).

3.4 Adsorption of iodine

PKSAC1, PKSAC2, PKSAC5 and NP, with decreasing V_{micro} are used to investigate the role of microporosity and the impact of larger mesopores in the adsorption of smaller adsorbates such as iodine. Figure 10 exhibits the adsorption capacity of the carbons by using different weight of activated carbons. Better performance is encountered for PKSAC1 than PKSAC2, PKSAC5 and NP, due to its higher

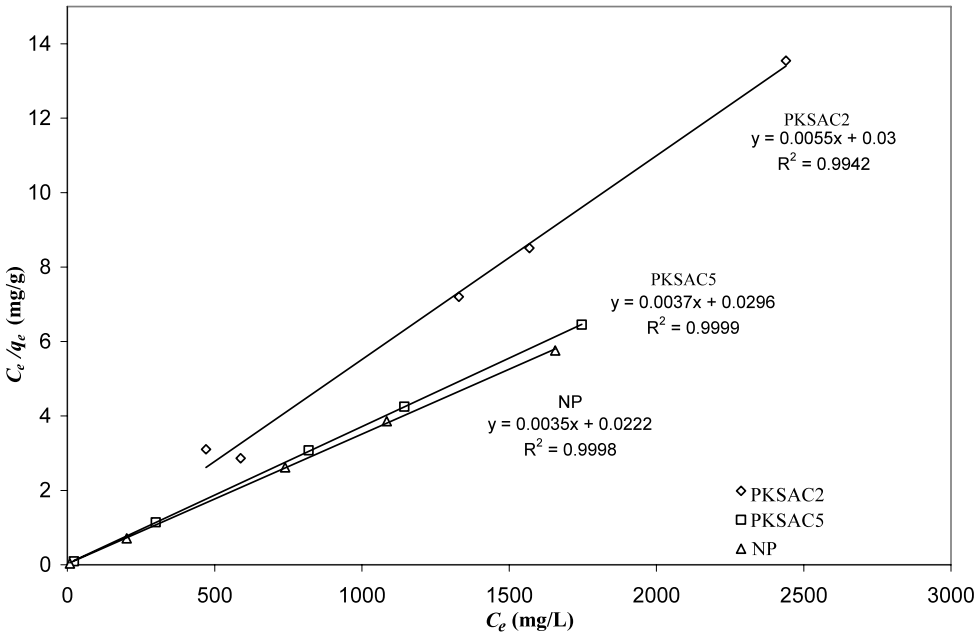

Fig. 9 Langmuir adsorption isotherms for PKSAC2, PKSAC5 and NP

Table 2 Comparative adsorption parameters of MB for PKSAC2, PKSAC5 and NP

	Langmuir Isotherm			Freundlich Isotherm			$\%V_{meso}/V_t$	S_{MB}	X_{MB}
	Q^0 mg/g	b l/mg	R^2	K_F mg/g(1/mg)$^{1/n}$	$1/n$	R^2		m^2/g	
PKSAC2	172.41	0.18	0.9942	136.98	0.040	0.0616	15.1	350.09	0.45
PKSAC5	263.16	0.13	0.9999	223.21	0.026	0.9731	44.1	534.36	0.64
NP	277.78	0.16	0.9998	232.39	0.030	0.8855	54.5	564.00	0.75

V_{micro}. On the contrary to MB adsorption, accessible microporosity becomes the main criterion rather than larger pores to yield better adsorption performances of small molecules. Therefore, the capillaries adjoined to the interior micropores of PKSAC structures may complimentary provide facilitative adsorption and diffusion of the iodine molecules.

3.5 Adsorption kinetics of MB

3.5.1 Kinetic models

Kinetic models of pseudo-first-order, pseudo-second and intraparticle diffusion model are employed to investigate the adsorption processes of the MB into the porous activated carbon structures. The integrated pseudo-first-order equation (Ho and McKay 1998; Wu et al. 2001) is given as,

$$\log(q_e - q_t) = \log q_e - k_f \cdot t/2.303 \tag{6}$$

where k_f (min^{-1}) is the rate constant of this model. The pseudo-second-order model (Ho and McKay 1998, 2000) can be expressed as

$$t/q_t = 1/k_s q_e^2 + t/q_e \tag{7}$$

where k_s ($\text{L mg}^{-1}\ \text{min}^{-1}$) is the rate constant of the second-order sorption model. This model predicts the adsorption behaviour over the whole range of adsorption and is in agreement with adsorption mechanism as the rate-controlling step (Otero et al. 2003).

Intraparticle diffusion model is based on the diffusion of adsorbates into the interior of the porous structures proposed by Weber and Morris (1963). The adsorption rate of the dye into the particle would depend on the rate of mass transport processes within the particle. The diffusion rate of the dye molecule, k_i, can be calculated from the linearised expression (Guibal et al. 1998; Wu et al. 2001),

$$q_t = k_i \cdot t^{0.5} \tag{8}$$

The extent of porosity generally governs the sorption kinetics of adsorbates depending upon the nature of both adsorbate and adsorbent. Kinetic models of pseudo-first order, pseudo-second-order and intraparticle diffusion have been employed to describe the sorption kinetic in PKSAC structures. The higher degree of mesoporosity in highly porous structures immensely promotes diffusion and adsorption of larger adsorbates (Banat et al. 2003; Gou et al. 2003; Juang

et al. 2000, 2002; Malik 2003; Métivier-Pignon et al. 2003; Tseng et al. 2003), hence, enhancing higher coverage in the interior micropores surface area.

The intraparticle diffusion model has been often applied in many physisorption studies in polydispersed structures, particularly activated carbons (Juang et al. 2000, 2002; Kannan and Sundaram 2001; Malik 2003). The adsorption phenomenon has been illustrated by the three stages of adsorbate diffusing into the interior of the structures. The gradual adsorption process in the second stage implies the rate-limiting step. However, the absence of multi-linearity plots in the PKSAC-MB systems concluded that multi-stages adsorption did not occur in the PKSAC structures (Fig. 11). In this study, the adsorption kinetics of MB into PKSAC2 and PKSAC5 preferably conforms to the pseudo-second-order model (Fig. 12) with high regression values ($R^2 > 0.992$) as compared to the pseudo-first-order (Fig. 13) and intraparticle diffusion models. This second-order kinetic behaviour suggests that the adsorption mechanism is the rate-controlling step. The calculated respective adsorption rate constants are enlisted in Table 3.

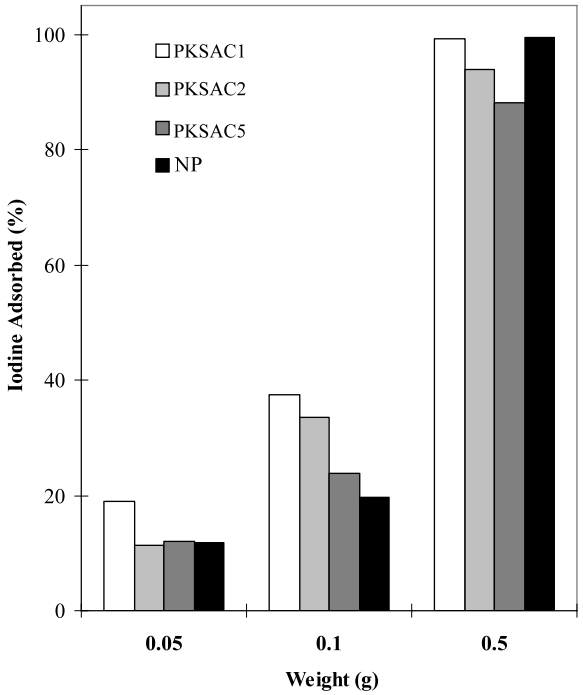

Fig. 10 Comparison on adsorption of iodine from 0.05 mol dm^{-3} I_2/KI solution between PKSAC1, PKSAC2, PKSAC5 and NP

3.6 Bleaching of glycerine

The performances of PKSAC2, PKSAC4 and PKSAC5 against SA and CA in the bleaching of glycerine are shown in Fig. 14. At lower weight fraction of 0.1, 0.5 and 1%, all activated carbons exhibited vast differences in the colour quality of the bleached glycerine. The influence of micro- and mesoporosity on the colour of bleached glycerine is crucial for all activated carbons. Lower dosage of PKSAC elucidated the limitations on the extent of nanoporosity on the final quality of the glycerine, where increasing performance of PKSAC is as follows; PKSAC5 > PKSAC4 and PKSAC2. However, at higher weight fraction of 1 and 5%, similar performances of all PKSAC and SA are achieved. CA is found to be ineffective due to its low microporosity as compared to SA and PKSAC.

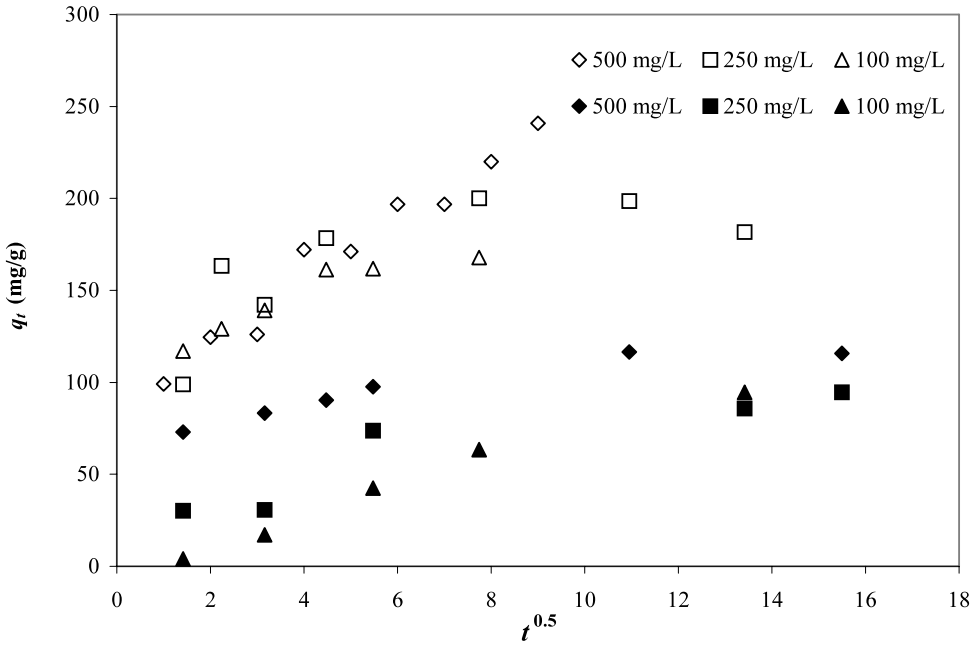

Fig. 11 Intraparticle diffusion model for the adsorption of MB on PKSAC2 (*filled*) and PKSAC5 (*non-filled*)

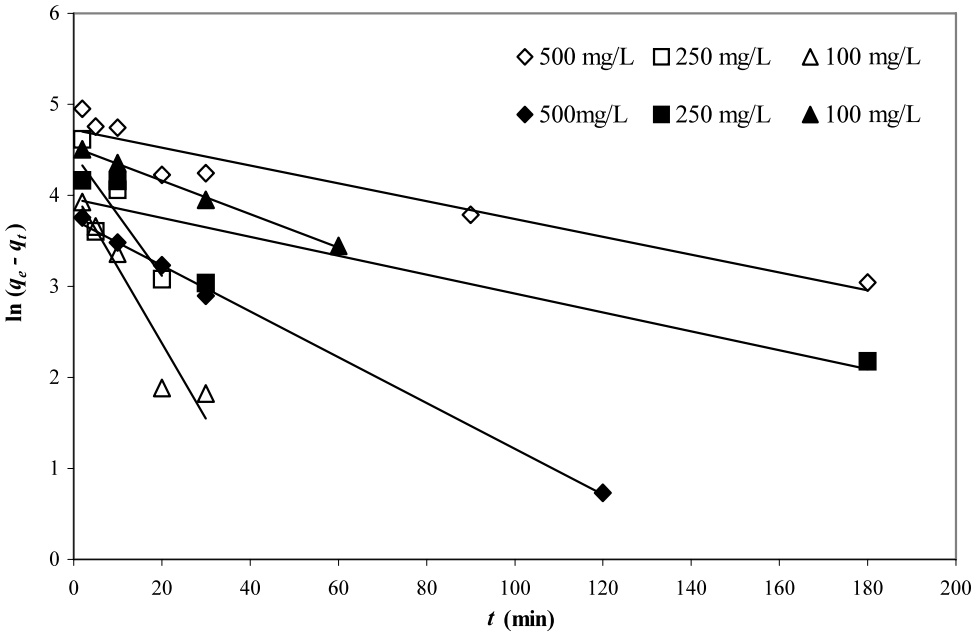

Fig. 12 Pseudo-first order model for the adsorption of MB on PKSAC2 (*filled*) and PKSAC5 (*non-filled*)

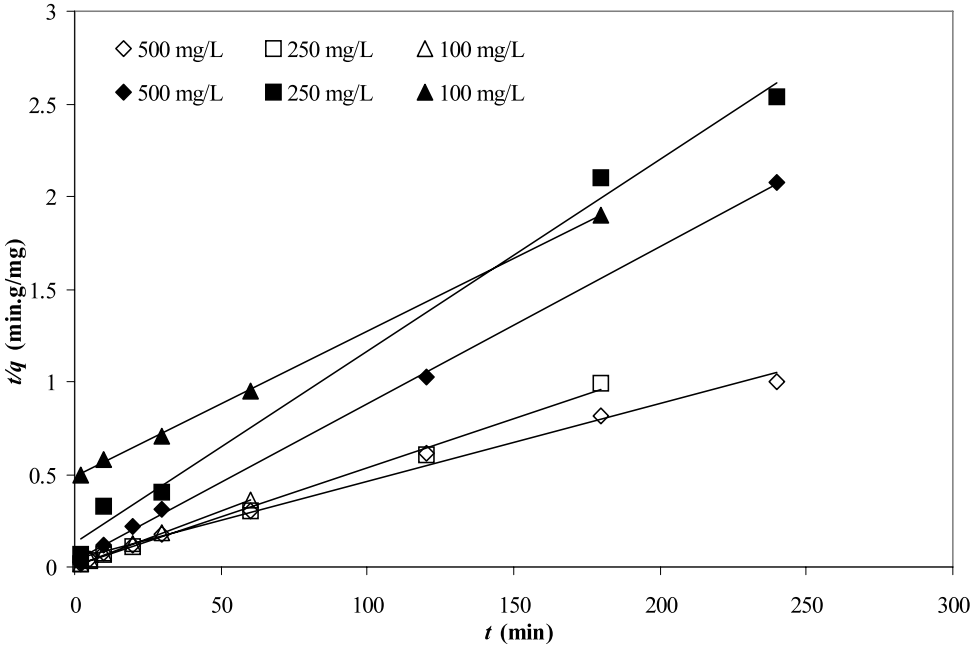

Fig. 13 Pseudo-second order model for the adsorption of MB on PKSAC2 (*filled*) and PKSAC5 (*non-filled*)

Table 3 Kinetic parameters for adsorption of MB at ambient temperatures on PKSAC2 and PKSAC5

C_0	Pseudo-first-order				Pseudo-second-order			
(mg L^{-1})	PKSAC2		PKSAC5		PKSAC2		PKSAC5	
	k_f 10^{-2} min^{-1}	R^2	k_f 10^{-2} min^{-1}	R^2	k_s 10^{-4} L mg^{-1} min^{-1}	R^2	k_s L mg^{-1} min^{-1}	R^2
100	4.24	0.9985	2.26	0.9141	1.25	0.9994	3.62e-03	0.9995
250	2.4	0.8124	15.57	0.6648	8.14	0.9935	1.4e-02	0.9962
500	5.8	0.9978	19.18	0.919	18.01	0.9994	4.47e-04	0.9916

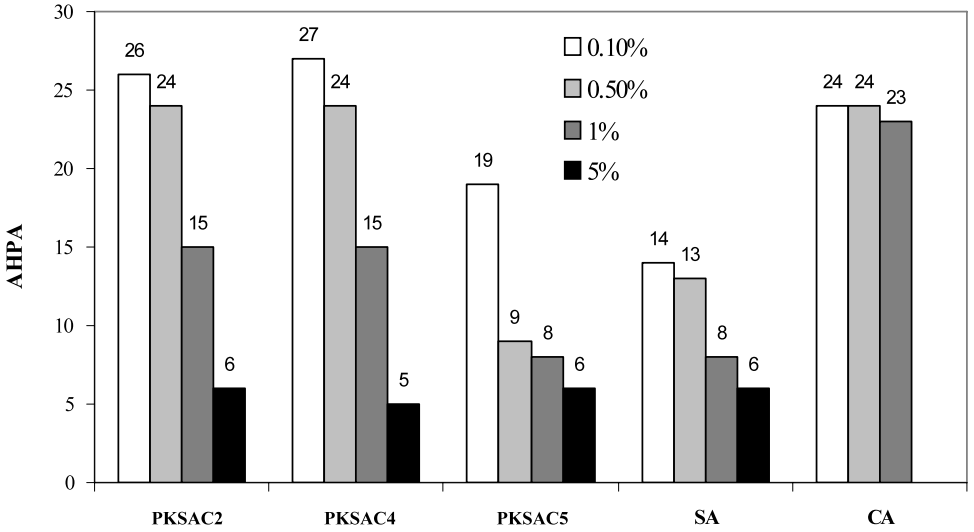

Fig. 14 Comparison on glycerine bleaching performance between PKSAC and other commercial activated carbons

4 Conclusions

Activated carbons derived from palm-kernel shells are characterized as highly porous materials with heterogeneous pore size distributions. The different extent of microporosity (68–79%) and mesoporosity (11–44%) in these structures implicated different adsorption behaviour towards adsorbates of different molecular sizes. The determination of the implications of micro- and mesoporosity and pore channelling effect in the PKSAC structures provide advantages in the processing designation of commercial processes. The unique structure and the distribution of micro and mesoporosity of the PKSAC materials that varied with particle size may be beneficially utilized in many novel applications. For instance, the adsorbent derived from palm kernel shell, particularly PKSAC5 exhibit high efficiency in the MB adsorption and colour bleaching in purification of glycerin. The performance of PKSAC5 in these two experiments is comparable to another commercial available activated carbon, NP. The adsorption can either be performed in batchwise in a batch stirred tank or continuous flow adsorption in a column. The spent adsorbent can be reused after reactivated either with heat (thermal recycling) or with steam (steam recycling).

Acknowledgements The work is financially supported by the Malaysian Palm Oil Board (MPOB). The authors also acknowledge the technical support of the Department of Chemical Engineering, Universiti Putra Malaysia. The helpful collaboration of KD Technology Sdn. Bhd. and AcidChem. (International) are gratefully acknowledged.

References

Banat, F., Al-Asheh, S., Al-Makhadmeh, L.: Evaluation of the use of raw and activated date pits as potential adsorbents for dye containing waters. Process Biochem. **39**, 193–202 (2003)

Barret, E.P., Joyner, L.G., Halenda, P.P.: The Determination of pore volume and area distributions in porous substances. I. Computations from nitrogen isotherms. J. Am. Chem. Soc. **73**, 373–380 (1951)

Brunauer, S., Emmet, P.H., Teller, F.J.: Adsorption of gases in multimolecular layers. J. Am. Chem. Soc. **60**, 309–319 (1938)

Chen, B., Hui, C.W., McKay, G.: Film-pore diffusion modeling and contact time optimization for the adsorption of dyestuff on pith. Chem. Eng. J. **84**, 77–94 (2001)

D'Silva, A.P.: Adsorption of antioxidants by carbon blacks. Carbon **36**, 1317–1325 (1998)

Do, D.D., Wang, K.: A new model for the description of adsorption kinetics in heterogeneous activated carbons. Carbon **36**, 1539–1554 (1998)

Dubinin, M.M.: Fundamentals of the theory of adsorption in micropores of carbon adsorbents: Characteristics of their adsorption properties and microporous structures. Carbon **27**, 457–467 (1989)

Gergova, K., Petrov, N., Minkova, V.: A comparison of adsorption characteristics of various activated carbons. J. Chem. Technol. Biotechnol. **56**, 77–82 (1993)

Gou, Y., Yang, S., Fu, W., Qi, J., Li, R., Wang, Z., Xu, H.: Adsoprtion of malachite green on micro- and mesoporous rice husk-based active carbon. Dyes Pigm. **56**, 219–229 (2003)

Gregg, S., Sing, K.S.W.: Adsorption Surface Area & Porosity. Academic Press, San Diego (1967)

Guibal, E., Milot, C., Tobin, J.M.: Metal-anion sorption by chitosan beads: equilibrium and kinetic studies. Ind. Eng. Chem. Res. **37**, 1454–1463 (1998)

Harkins, W.D., Jura, G.: Surfaces of Solids. XIII. A vapor adsorption method for the determination of the area of a solid without the assumption of a molecular area, and the areas occupied by nitrogen and other molecules on the surface of a solid. J. Am. Chem. Soc. **66**, 1366–1373 (1944)

Ho, Y.S., McKay, G.: Comparative sorption kinetic studies of dye and aromatic compounds onto fly ash. J. Environ. Sci. Health A **34**, 1179–1204 (1998)

Ho, Y.S., McKay, G.: The kinetics of sorption of divalent metal ions onto sphagnum moss peat. Water Res. **34**, 735–742 (2000)

Hsieh, C.-T., Teng, H.: Influence of mesopore volume and adsorbate size on adsorption capacities of activated carbons in aqueous solutions. Carbon **38**, 863–869 (2000)

Hu, X., Do, D.D.: Effect of surface heterogeneity on the sorption kinetics of gases in activated carbon, pore size distribution versus energy distribution. Langmuir **10**, 3296–3302 (1994)

Juang, R.S., Wu, F.C., Tseng, R.L.: Mechanism of adsorption of dyes and phenols from water using activated carbons prepared from plum kernels. J. Colloid Interface Sci. **227**, 437–444 (2000)

Juang, R.S., Wu, F.C., Tseng, R.L.: Characterization and use of activated carbons prepared from bagasses for liquid-phase adsorption. Colloids Surf. A **201**, 191–199 (2002)

Kaewprasit, C., Hequet, E., Abidi, N., Gourlot, J.P.: Application of methylene blue adsorption to cotton fiber specific surface area measurement: Part I. Methodology. J. Cotton Sci. **2**, 164–173 (1998)

Kannan, N., Sundaram, M.M.: Kinetics and mechanism of removal of methylene blue by adsorption on various carbons—A comparative study. Dyes Pigm. **51**, 25–40 (2001)

Kluson, P., Scaife, S.J.: Pore size distribution analysis of structure different microporous carbons-theoretical evaluation based on density functional theory and nitrogen and argon experimental adsorption isotherms at 77 K. Chem. Biochem. Eng. **15**, 117–125 (2001)

Laurendeau, N.M.: Heterogeneous kinetics of coal char gasification and combustion. Prog. Energy Combust. Sci. **4**, 221–270 (1978)

Luo, A.C., Guo, J.: Microporous oil-palm-shell activated carbon prepared by physical activation for gas-phase adsorption. Langmuir **17**, 7112–7117 (2001)

Luo, A.C., Guo, J.: Surface functional groups on oil-palm-shell adsorbents prepared by H3PO4 and KOH activation and their effects on adsorptive capacity. Chem. Eng. Res. Des. **81**, 585–590 (2003)

Luo, A.C., Jia, Q.: Adsorption of phenol by oil-palm-shell activated carbons. Adsorption **13**, 129–137 (2007)

McKay, G., Porter, J.F., Prasad, G.R.: The removal of dye colours from aqueous solutions by adsorption of low-cost materials. Water Air Soil. Pollut. **114**, 423–438 (1999)

Malik, P.K.: Use of activated carbons prepared from sawdust and rice-husk for adsorption of acid dyes: A case study of acid yellow 36. Dyes Pigm. **56**, 239–249 (2003)

Métivier-Pignon, H., Faur-Brasquet, C., Le Cloirec, P.: Adsorption of dyes onto activated carbon cloths: Approach of adsorption mechanisms and coupling of ACC with ultrafiltration to treat coloured wastewaters. Sep. Purif. Technol. **31**, 3–11 (2003)

Otero, M., Rozada, F., Calvo, L.F., Garciá, A.I., Morán, A.: Kinetic and equilibrium modelling of the methylene blue removal from solution by adsorbent materials produced from sewage sludges. Biochem. Eng. J. **15**, 59–68 (2003)

Pelekani, C., Snoeyink, V.L.: Competitive adsorption in natural water: Role of activated carbon pore size. Water Res. **33**, 1209–1219 (1999)

Prasetyo, I., Do, H.D., Do, D.D.: Surface diffusion of strong adsorbing vapours on porous carbons. Chem. Eng. Sci. **57**, 133–141 (2002)

Pritzker, M.D.: Model for parallel surface and pore diffusion of an adsorbate in a spherical adsorbent particle. Chem. Eng. Sci. **58**, 473–478 (2003)

Safanova, A.M., Luneva, N.K., Vasiliev, L.L., Mishkinis, D.A.: Activated carbons for gas adsorption. In: IV International Seminar on Heat Pipes, Heat Pumps, Refrigerators, Minsk, Belarus (2000)

Sircar, S., Golden, T.C., Rao, M.B.: Carbon for gas separation and storage. Carbon **34**, 1–12 (1996)

Tan, I.A.W., Ahmad, A.L., Hameed, B.H.: Adsorption of basic dye using activated carbon prepared from oil palm shell: batch and fixed bed studies. Desalination **225**, 13–28 (2008)

Teng, H., Hsieh, C.T.: Influence of surface characteristics on liquid-phase adsorption of phenol by activated carbons prepared from bituminous coal. Ind. Eng. Chem. Res. **37**, 3618–3624 (1998)

Tien, C.: Adsorption Calculations and Modelling. Butterworth-Heneimann, Newton (1994)

Tseng, R.L., Wu, F.C., Juang, R.J.: Liquid-phase adsorption of dyes and phenols using pinewood-based activated carbons. Carbon **41**, 487–495 (2003)

Weber, W.J., Morris, J.C.: Kinetics of adsorption on carbon from solution. J. Sanit. Eng. Div. Am. Soc. Civ. Eng. **89**, 31–60 (1963)

Wu, F.C., Tseng, R.L., Juang, R.S.: Kinetic modeling of liquid-phase adsorption of reactive dyes and metal ions on chitosan. Water Res. **35**, 613–618 (2001)

Yang, O.B., Kim, J.C., Lee, J.S., Kim, Y.G.: Use of activated carbon fiber for direct removal of iodine from acetic acid solution. Ind. Eng. Chem. Res. **32**, 1962–1697 (1993)